RESOLUTION MEASUREMENTS OF HIGH ENERGY RADIOGRAPHY

Y. Bushlin, Y. Segal, and A. Notea

Quality assurance and Reliability, Technion
Haifa 32000, Israel

INTRODUCTION

The resolution of a film or film - screen combination is essential for characterizing the radiographic system. The conventional methods for measuring the resolution in radiography, based on the Image Quality Indicators (IQI) and Penetrameters, are not applicable for high energy radiation (in the MV range) due to the high penetration. In addition, the IQI and Penetrameters do not measure only the spatial resolution but rather an undefined combination of the spatial and thickness resolution. Another approach used for analyzing the film resolution is based on the measurement of the radiographic response to a step function input. Under the assumption that radiography is mathematically described by a linear and shift invariant system [1] the image is expressed by the transformation of the 'ideal image' $O_i(x)$ to the measured image $O_m(x)$ via the convolution with a characteristic function (the Line Spread Function LSF, in the one dimensional case):

$$O_m(x) = \int_{-\infty}^{\infty} O_i(x')LSF(x - x')dx' \tag{1}$$

whenever $O_i(x)$ is a step change the LSF can be derived from eq.1 by:

$$LSF(x) = \frac{1}{H}\left|\frac{dO_m(x)}{dx}\right| \tag{2}$$

where H is the step height in density units.

This study shows that the determination of the LSF from the response $O_m(x)$ to the step is not a straightforward process. A more general approach [2] was applied for the solution of the radiographic inverse problem. The modelling developed refers to all major effects that influence the image generation process.

THE EXPERIMENTAL SETUP

The radiation source was a 9MV linear accelerator, Linac 3000 (Varian Ltd.). The step wedges used were steel blocks with lateral dimensions of 20×15 cm and 20×30 cm with various heights.

Review of Progress in Quantitative Nondestructive Evaluation, Vol. 9
Edited by D.O. Thompson and D.E. Chimenti
Plenum Press, New York, 1990

Due to the high sensitivity of the obtained image [3] to the inclination angle between the radiation beam and the step edge a special alignment system was built (Fig.1). The focus to film distance was 10 meters to ensure a uniform field intensity distribution on the entire wedge block. The steps were placed at least 3 meters from any wall to diminish the effect of backscatterd radiation. Exposures were taken with different combinations of film and Pb screens, step base height and at various radiation intensities to yield a wide range of film densities and exposure geometries.

The obtained radiographs were digitized by an automatic microdensitometer (Photomation 1700; Optronics Ltd.) with an aperture of $50 \times 50\mu m$. To improve the signal to noise ratio, 600 lines (read perpendicular to the step edge line) were averaged.

ANALYSIS OF THE MEASURED DENSITY PROFILES

Implementation of eq.2 to noisy data may yield erroneous results. Therefore an iterative algorithm for inverse problem solution was chosen for characterizing the LSF out of the measured steps profiles. This algorithm is based on a theoretical model for the step response that is least squares fitted to the measured profile. The response model in this study is based on eq.1 and on an exponential LSF [4]. Hence the theoretical step profile is given by:

$$\begin{aligned} O_t(x) &= H[h(x-x_0)] * \tfrac{\lambda}{2}\exp^{-\lambda|x|} \\ &= \tfrac{H}{2}[1 + \tfrac{x-x_0}{|x-x_0|}(1-\exp^{-\lambda|x-x_0|})] \end{aligned} \tag{3}$$

where x_0 is the step edge position and λ is the blurring parameter which is related to the LSF full width at half maximum (fwhm) by:

$$fwhm = \frac{2\ln 2}{\lambda} \tag{4}$$

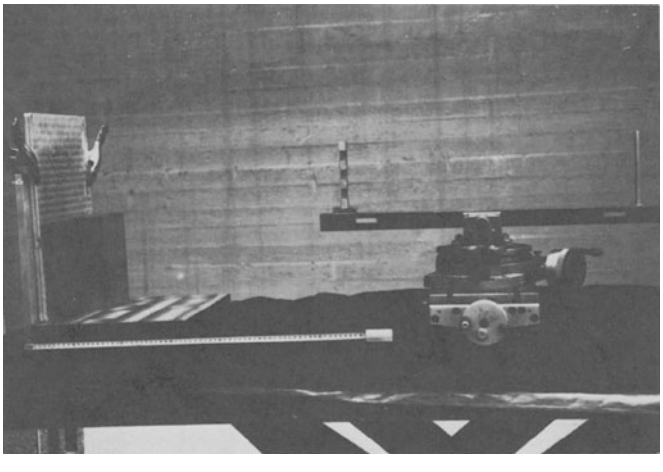

Figure 1. Alignment system and the steel step wedge. When the image of the rod coincide with the edge of the image of the rectangular shaped blocks, the focal spot is aligned with these two objects. The two objects are placed on an accurate rotational table connected to an x-y table.

In Fig.2 fitted profiles, eq.3, are shown together with the measured ones. It is clearly seen that as the analysis involves larger portions of the profile on both sides of the edge the fit is less satisfactory. The measured data tends to reach a saturation level further from the edge than the calculated response. This effect was discussed in previous publications [5,6] and attributed to the contribution of the scattered photons generated within the volume of the steel blocks. The scattered photons effect results in a "cap" curvature in the profile, and the step response is superimposed on it. As was demonstrated in [5] the "cap" curvature turns the step response to be position dependent. The long distance influence of the curvature will affect the measured fwhm. As the number of pixels around the edge involved in the analysis increases, the "cap" curvature influence also increases and the resulted LSF becomes wider, see Fig.3. This behavior was obtained also with other functions for the LSF such as the arctan [7]:

$$O_t(x) = H \arctan(\lambda_a(x - x_0)) \tag{5}$$

and a combination of the exponential LSF with an impulse function [8]:

$$O_t(x) = \frac{H}{2}[1 + \frac{x - x_0}{|x - x_0|}(1 - \frac{2b}{\lambda_\delta} \exp^{-\lambda_\delta|x-x_0|})] \tag{6}$$

Therefore a proper modelling of the radiographic process should include the curvature effect. In previous works [2,3,5,6] a semi-empirical and phenomenological approach to describe the image generation process was presented. Following this approach the radiographic image generation i.e. the direct problem, is expressed by two types of operators representing the various effects. The first type is the linear and shift invariant characteristic function (LSF) while the second may be a non linear and local dependent operator. The "cap" curvature effect was described by a polynomial operator P [5]. Based on the operator presentation the measured image is given by:

$$O_m(x) = L_{x-x'} P_x k[i(\xi)] \tag{7}$$

where $i(\xi)$ is the mathematical description of the examined block wedge and k is an operator transforming from radiation chord length units to optical density. The determination of the LSF parameters by fitting O_t of eq.3 to the measured profile should be done following the application of the inverse operator P^{-1}.

Whenever it is not possible to find a proper polynomial description for P the fitting of eq.3 should be carried out only in a close vicinity of the edge in order to diminish the influence of the long term curvature effect. That is the reason that the fitting is quite satisfactory for short profiles, see Fig.2. The χ^2criterion was used as an objective criterion for the profile length. The criterion states that the best fit will yield the smallest value of the mean square error (MSE):

$$MSE = \frac{1}{(N - 1 - N_p)} \sum_{i=1}^{N} [O_t(i) - O_m(i)]^2 \tag{8}$$

where N is the number of pixels and N_p is the number of fitting parameters.

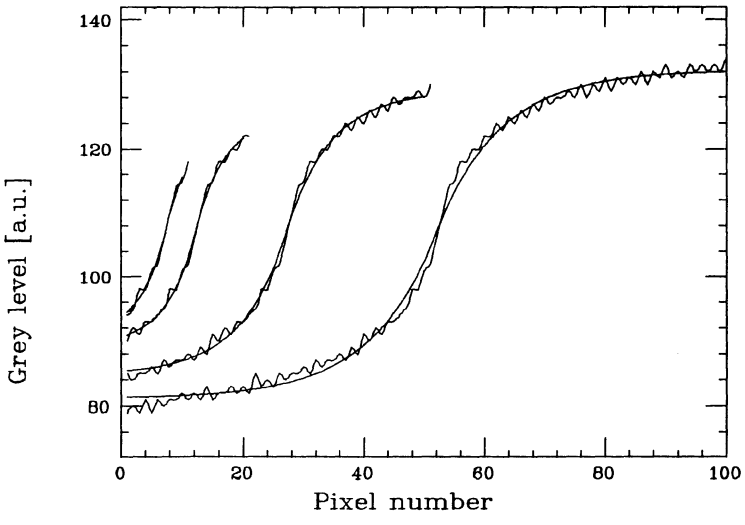

Figure 2. Measured and fitted (smooth curves) profiles for a stainless steel step wedge composed of two blocks 20 x 15 x 2cm over 20 x 30 x 2cm radiographed at 9 MV using film D7 and 0.1mm Pb screen. Digitization aperture 50 μm. Profiles length: 10, 20, 50, 100 pixels.

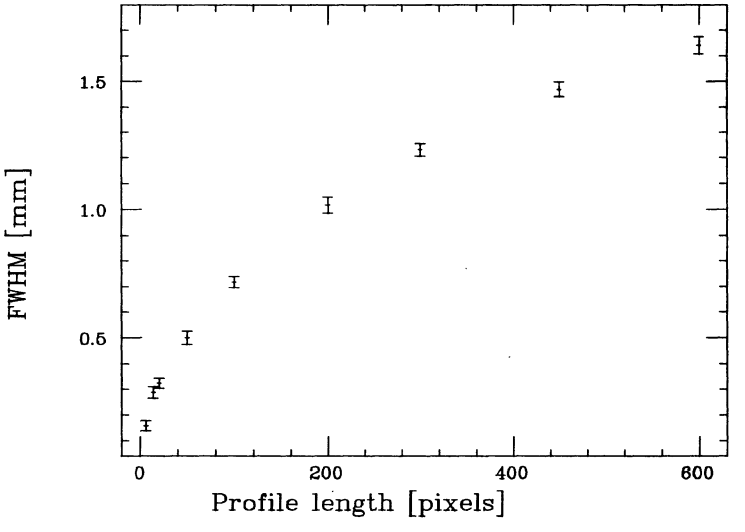

Figure 3. FWHM of the exponential LSF as function of the profile length, obtained by fitting of Eq. 3 to the measured film density of the step described in Figure 2.

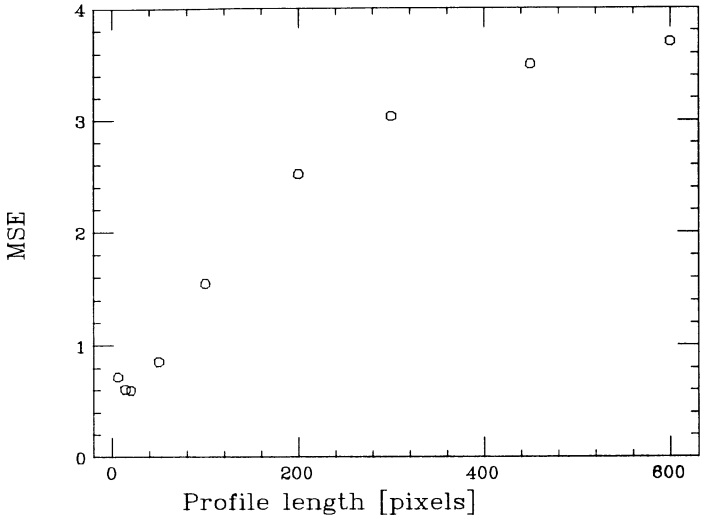

Figure 4. The mean square error in fitting Eq. 3 to the measured film density profiles of the step from Fig. 2. The minimum in the MSE was obtained for a profile length of 20 pixels.

As N increases, the data is more influenced by the "cap" curvature effect, eq.3 does not describe the $P_x k[i(\xi)]$ profile and the MSE increases. From eq.8 it is clear that the MSE increases as N decreases, and therefore for a certain N a minimum value is obtained, see Fig.4.

Using the χ^2criterion for the optimal choice of the profile length, eq.3 was applied for determining the fwhm of the LSF for all the step wedges that were radiographed. The data obtained from the radiographic images was used for parameter analysis study. Some of the results are presented in Tables 1 to 4. The width of the LSF presented in the tables serves as a measure for the resolution. In some cases it is more convenient to use the cut-off frequency w_c of the MTF (Modulation Transfer Function) as a measure. The transformation of fwhm to w_c (for exponential LSF) is given by:

$$w_c = \frac{2\ln 2}{fwhm}\sqrt{M_0^{-1} - 1} \tag{9}$$

where M_0 is the threshold modulation.
For example, fwhm of 0.5mm appears for threshold modulation of 2% as a cut-off frequency of $20[lines/mm]$.

CONCLUSIONS

From the results presented in Tables 1 to 4 the following points should be stressed:

The spatial resolution obtained with film D4 is better than with Film D7 (Table 1). This result was expected due to the finer grains

Table 1. Influence of film type on the *fwhm* of the LSF. The values were obtained by least squares fitting of eq.3 to the measured density profiles of a stainless steel step wedge radiographed with a $9MV$ linear accelerator. The radiographs were digitized with an aperture of $50\mu m$ and 600 lines were averaged. The χ^2 criterion was applied to determine the profile length. Values of the last column were obtained using profile lengths of 50 pixels.

Film type	Pb screen $[mm]$	Base/ step height $[mm]$	Film density $[D]$	Profile length $[pixels]$	$FWHM$ $[mm]$	$FWHM$ for 50 pixels
D7	0.1	20/20	1.63/2.60	20	0.32	0.50
D4	0.1	20/20	1.66/2.45	10	0.26	0.60
D7	0.1	40/20	1.16/1.64	50	0.80	0.80
D4	0.1	40/20	1.13/1.72	14	0.64	0.90

Table 2. Influence of film density on the *fwhm* of the LSF. (The analysis performed is the same as in Table 1.)

Film density $[D]$	Pb screen thickness $[mm]$	Base height/ step height $[mm]$	Film type	Profile length $[pixels]$	$FWHM$ $[mm]$
1.07/1.55	0.1	20/20	D4	50	0.61
1.66/2.45	0.1	20/20	D4	10	0.26
0.61/0.89	0.1	40/20	D4	50	0.98
1.13/1.72	0.1	40/20	D4	10	0.64
0.36/0.51	0.1	60/20	D4	450	2.93
0.61/0.89	0.1	60/20	D4	1015	1.02

Table 3. Influence of Pb screen on the *fwhm* of the LSF. (The analysis performed is the same as in Table 1.)

Pb screen thickness $[mm]$	Film density $[D]$	Base height/ step height $[mm]$	Film type	Profile length $[pixels]$	$FWHM$ $[mm]$
0.1	1.63/2.30	20/20	D7	20	0.33
---	1.86/2.60	20/20	D7	10	0.35
0.7	1.11/1.59	40/20	D7	20	0.30
---	1.39/2.00	40/20	D7	20	0.40
0.7	1.11/1.59	40/20	D7	20	0.30
0.1	1.16/1.64	40/20	D7	50	0.80
0.7	0.38/0.54	40/20	D4	50	0.53
0.1	0.61/0.89	40/20	D4	100	0.98

Table 4. Influence of base height on the $fwhm$ of the LSF. (The analysis performed is the same as in Table 1.)

Base height/ step height $[mm]$	Film density $[D]$	Pb screen thickness $[mm]$	Film type	Profile length $[pixels]$	$FWHM$ $[mm]$
20/20	1.07/1.55	0.1	D4	50	0.61
40/20	1.13/1.72	0.1	D4	14	0.64
40/20	0.61/0.89	0.1	D4	100	0.98
60/20	0.61/0.89	0.1	D4	100	1.02

of D4, however, when the χ^2criterion is not used an opposite result is obtained.

A higher film density will result with a better resolution (Table 2). This can be explained by the behavior of the gradient curve of the characteristic film function.

The presence of the Pb screen improves the resolution (Table 3). The 0.7mm screen gave smaller fwhm. This result indicated that in the MV range radiography the screen is acting as filter for the low energy scattered photons.

From Table 4 it is clear that the step base height has no influence on the measured value of the fwhm (in the height range that was tested). This is encouraging since it indicates that the obtained results are independent of the specific step that was used for the measurement.

ACKNOWLEDGMENT

The study was supported by the Land Niedersachsen (Niedersachsisches Ministerium fur Wissenschaft and Kunst) W. Germany.

REFERENCES

1. G.E. Metz and K. Doi, Phys. Med. Bio., 24, p.1079 (1979).
2. A. Notea, NDT International 21 p.379 (1988).
3. Y.Bushlin, and A. Notea, NDT International 21 p.397 (1988).
4. A. Fishman, U. Feldman, A. Notea, and Y. Segal, Materials Evaluation 41, p.1201 (1983).
5. U. Feldman, Y. Bushlin, and A. Notea, NDT International 21 p.415 (1988).
6. A. Notea, Y. Bushlin, U. Feldman, in J. Boogaard and G. M. Van Dijk (ed.s) Non-Destructive Testing (Proc. 12th world conf.) Elsavier Science Pub. Amsterdam, p.1084 (1989).
7. M.F. Sulcoski, K.W. Tobin, and J.S. Brenizer, Nuclear Technology, 82, p.355 (1988).
8. A. Notea and Y. Segal, Nuclear Technology, 63, p.121 (1983).